**Academic Journal of Architecture and Civil Engineering**
**ISSN: 2960-0235**
**DOI: 10.61784/ajace3007**

# STUDY ON THE MODIFICATION OF EARTH PRESSURE DISTRIBUTION PATTERN OF CIRCULAR WORKING SHAFT IN SOFT SOIL AREA

Lei Wu[1, 2], ZhiCheng Bai[1, 2*], MinJian Long[1, 2], XiaoXia Zhao[1, 2], ZhiYuan Zhang[1, 2], HuiZhou Ni[1, 2]
[1]*China Construction Fourth Engineering Bureau Co., Ltd. Guangzhou 510000, Guangdong, China.*
[2]*China Construction Fourth Engineering Bureau Sixth Construction Co., Ltd. Hefei 230000, Anhui, China.*
*Corresponding Author: ZhiCheng Bai, Email: 19822660870@163.com*

**Abstract:** This article relies on actual engineering projects to conduct research on the earth pressure distribution model of circular working wells in soft soil areas. By establishing a well-soil three-dimensional numerical analysis model, the lateral displacement of the working well enclosure in the soft soil area is analyzed, and the earth pressure calculation method that considers the displacement effect is used to analyze the lateral earth pressure of the enclosure. On this basis, the influence of the working well space arch effect on the earth pressure distribution pattern under the conditions of wall insertion ratio, working well radius, wall thickness, wall elastic modulus and other factors was analyzed. Subsequently, based on the existing specifications, the soil pressure distribution model of circular working wells in soft soil areas was revised. The study shows that the radius of the working well has a significant impact on the earth pressure distribution pattern; in addition, the study obtained a fitting formula for the starting and ending depth and radius of the earth pressure reduction of the circular working well; and through comparative analysis, it was found that the use of considering the circular arch The effect-corrected earth pressure plane foundation beam method is simpler than the three-dimensional finite element method, has more mature parameter selection, and has lower calculation costs. Compared with the plane elastic foundation beam method of standardized earth pressure, it is closer to the actual displacement direction.
**Keywords:** Soft soil area; Circular working well; Spatial arch effect; Earth pressure distribution model

## 1 INTRODUCTION

Foundation pit engineering is a complex systematic project. The influence of many factors such as the stability of the supporting structure, the strength of the soil, the engineering environment and the seepage of groundwater has brought great challenges to the design and construction of foundation pit engineering. Tang Yeqing et al. [1] collected more than 160 cases of foundation pit engineering accidents. Most of the accidents were caused by inaccurate calculation of soil pressure. With the acceleration of urbanization in my country and the increasing development and utilization of underground space, the number of foundation pit projects is increasing. The circular foundation pit has the following two advantages: first, the retaining structure of the foundation pit will form a circular whole. This closed arch structure can make the retaining structure have the characteristics of circumferential compression, thereby giving full play to the high compressive strength of concrete materials [2]; second, the soil outside the circular foundation pit can produce an obvious "soil arch" effect, making the soil pressure acting on the circular support structure less than that of the straight-sided foundation pit. Therefore, more and more foundation pits are now using circular structure design [3]. At present, there are few literatures on the study of soil pressure in circular foundation pits. The research methods are mainly limited to the limit equilibrium method and the slip line method. The results obtained are only applicable to the ideal situation where the soil is uniform, the ground surface is horizontal, and the wall is vertical and smooth. Berezantzev[4] assumed that the hoop stress is equal to the first principal stress, derived the limit equilibrium differential equation under the three-dimensional axisymmetric case, and solved it using the slip line method, solving the problem of soil pressure in circular foundation pits under ideal conditions. Prater[5] summarized the limit equilibrium solution of active earth pressure in circular foundation pits, introduced the hoop stress coefficient, and analyzed its influence on soil pressure. The research results show that the soil pressure will decrease with the increase of the hoop stress coefficient, and it is recommended to take the hoop stress coefficient as the static earth pressure coefficient in actual calculations. Cheng et al.[6] introduced the hoop stress coefficient based on Prater's theory, assumed that the slip line is two sets of parallel straight lines, and solved the simplified slip line solution of the circular shaft soil pressure. They proposed that the result obtained by the Berezantzev solution, that is, when the hoop stress coefficient is 1.0, is too dangerous, and suggested that the hoop stress coefficient be taken according to the static soil pressure coefficient K0. Liu Faqian[7], based on the slip line theory, considered the influence of multiple factors such as the friction angle between the wall and the soil, the distribution of the pile load, the ground slope and the groundwater seepage on the soil pressure, and systematically studied the soil pressure acting on the circular foundation pit retaining structure; based on the limit analysis theory, the energy dissipation caused by the hoop compression of the soil was considered, and the upper limit solution of the active soil pressure of the circular foundation pit was derived, further developing the soil pressure theory. Zai Jinmin[8-10] et al. proposed a new method for calculating the soil pressure of the retaining wall. This method comprehensively considers the deformation of the wall and the change of the soil pressure. Lu Guosheng[11] et al. considered the influence of displacement when calculating the soil pressure, and compared the results with the finite element calculation results. Chen Yekai [12-14] used an exponential function to describe the relationship between the earth pressure acting on the retaining wall and the wall displacement, and calculated the earth pressure acting on the retaining wall under the non-limit state.

The theoretical research results of the earth pressure of circular foundation pits are still incomplete. The earth pressure results obtained based on the plane assumption do not consider the influence of factors such as the spatial effect of the soil and the curvature radius of the foundation pit. When the limit equilibrium method is used, the distribution form of the earth pressure cannot be obtained according to the static equilibrium of the sliding wedge. When the slip line method is used, it is necessary to properly describe the annular stress of the circular foundation pit, but the existing research results do not have a clear understanding of the annular stress of the soil around the circular foundation pit.

Based on the municipal comprehensive renovation project of Shanghai Hongqiao Business District, this paper intends to carry out a study on the earth pressure distribution pattern of circular working wells in soft soil areas. Based on the large-scale general finite element software Abaqus, a well-soil three-dimensional numerical analysis model is established. Considering factors such as wall insertion ratio, working well radius, wall thickness, and wall elastic modulus, the influence of the spatial arch effect of the working well on the earth pressure distribution pattern is explored. Based on the existing Shanghai Engineering Construction Code "Technical Code for Foundation Pit Engineering" [15], the soil pressure distribution model of circular working wells in soft soil areas is proposed and verified by combining engineering examples.

## 2 PROJECT OVERVIEW

The Shanghai Hongqiao Business District Municipal Comprehensive Renovation Project is located in a soft soil area and includes 2 working wells, 2 receiving wells and a water inlet gate well. Among them, the 4# working well is a circular structure with a diameter of 14m and a depth of 15m. It is a deep and large foundation pit with high requirements for its safety and stability. The outer side of the shaft is composed of a double-row bored cast-in-place pile water-stop curtain to form a retaining structure. The cast-in-place pile is 23m long and the wall is 1.5m thick. The working well is not supported and is constructed by layered reverse construction. The shaft excavation is divided into three steps. The specific construction conditions are shown in Table 1. The basic soil layer parameters are shown in Table 2.

**Table 1** Construction Conditions

| Working condition | Excavation depth and lining casting |
|---|---|
| Working condition 1 | 5m, casting lining within the depth range of 0-5m |
| Working condition 2 | 10m, casting lining within the depth range of 5-10m |
| Working condition 3 | 15m, casting lining and bottom plate within the depth range of 10-15m |

**Table 2** Basic Soil Layer Parameters

| Serial number | Soil layer | thickness（m） | Severe$\gamma$（kN/m$^3$） | Initial porosity $e_0$ | Cohesion $c$（kPa） | Poisson's ratio $v$ |
|---|---|---|---|---|---|---|
| 1 | Clay soil | 2.3 | 18.82 | 0.94 | 15 | 0.47 |
| 2 | Silty clay soil | 5.6 | 17.85 | 1.18 | 17 | 0.35 |
| 3 | Silty clay soil | 6.9 | 17.15 | 1.43 | 16 | 0.4 |
| 4 | Brown clay soil | 7.3 | 18.25 | 1.03 | 15 | 0.35 |
| 5 | Green clay soil | 1.8 | 19.8 | 0.71 | 15 | 0.3 |
| 6 | Silty sand | 21 | 19.25 | 0.76 | 6.7 | 0.3 |
| 7 | Clay mixed with silty sand | 33 | 18.45 | 0.94 | - | 0.61 |

## 3 THREE-DIMENSIONAL FINITE ELEMENT ANALYSIS MODEL OF WELL-SOIL INTERACTION

### 3.1 Finite Element Analysis Model

Based on the critical state theory and triaxial tests of weakly overconsolidated soil and normally consolidated soil, Roscoe et al. [16] of Cambridge University proposed the Cambridge model (CCM). Later, Roscoe et al. [17] modified the bullet-shaped yield surface of the Cambridge model and obtained the modified Cambridge model (MCC Model). The modified Cambridge model describes the elastic-plastic deformation characteristics of soil well both theoretically and experimentally, and is one of the most widely used soft soil constitutive models.

The modified Cambridge model requires four calculation parameters [17], namely the slope λ of the normal consolidation line in the v-lnp' plane, the slope k of the rebound line in the v-lnp' plane, the slope M of the CSL on the p'-q' plane, and the Poisson's ratio v. Among them, λ, k, and M can be obtained according to the following formula:

$$\lambda = \frac{C_c}{\ln 10} \tag{1}$$

$$k = \frac{C_s}{\ln 10} \tag{2}$$

$$M = \frac{6\sin\varphi'}{3-\sin\varphi'} \quad (3)$$

In the formula, $C_C$ is the compression index of the soil, $C_S$ is the rebound index of the soil, and φ' is the effective internal friction angle obtained from the triaxial compression test.

This paper adopts the Coulomb friction model with limited sliding to simulate the friction between the surrounding structure and the soil. In the Coulomb friction model, before starting to slide against each other, the two contact surfaces generate equivalent shear stress $\tau_{equal}$ on their interface:

$$\tau_{equal} = \sqrt{\tau_{FS1}^2 + \tau_{FS2}^2} \quad (4)$$

In the formula, $\tau_{FS1}$ is the shear (friction) stress in the 1st direction on the contact surface; $\tau_{FS2}$ is the shear (friction) stress in the 2nd direction on the contact surface.

The critical shear stress $\tau_{crit}$ is proportional to the normal contact stress P, as shown below:

$$\tau_{crit} = \mu P \quad (5)$$

In the formula, μ is the friction coefficient.

Setting the limit shear stress for the critical shear stress $\tau_{crit}$, the critical shear stress can be expressed as:

$$\tau_{crit} = \min(\mu P, \tau_{max}) \quad (6)$$

Wherein, $\tau_{crit}$ is the limit shear stress. For the problem of the interaction between the underground continuous wall and the soil, $\tau_{max}$ is equivalent to the limit side friction resistance of the underground continuous wall.

When the equivalent shear stress $\tau_{equal}$ on the contact surface exceeds the critical shear stress $\tau_{crit}$, relative sliding begins to occur between the contact surfaces, as shown in Figure 1.

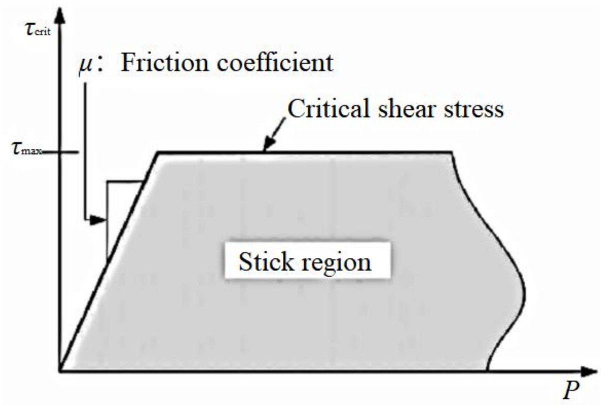


**Figure 1** Coulomb Friction Characteristics [17]

Table 3 lists the basic calculation parameters of typical soil layers in soft soil areas, among which the effective internal friction angle φ', lateral pressure coefficient K0, compression curve slope λ, rebound curve slope k, critical state parameter M, and Young's modulus E can be obtained according to the above formula and relevant literature.

The contact surface parameters include the ultimate lateral friction resistance $\tau_{max}$ of the continuous wall and the wall-soil friction coefficient μ, among which $\tau_{max}$ refers to the standard value of the ultimate lateral friction resistance of cast-in-place piles in the "Geotechnical Engineering Investigation Code" [18], and the wall-soil friction coefficient μ refers to the recommended value of the friction coefficient between the pile foundation base and the foundation soil in the National Technical Code for Building Pile Foundations [19]. See Table 4 for details.

**Table 3** Basic Calculation Parameters of Typical Soil Layers in Soft Soil Areas

| Serial number | Effective internal friction angle $\psi'$（°） | Side pressure coefficient $K_0$[20] | Compression curve slope $\lambda$[21-22] | Rebound curve slope $k$[23] | Critical state parameters $M$ | Young's modulus $E$（MPa）[24] |
|---|---|---|---|---|---|---|
| 1 | 32 | 0.3 | 0.12 | 0.01 | 0.6 | - |
| 2 | 29 | 0.52 | 0.1 | 0.008 | 0.55 | - |
| 3 | 18 | 0.69 | 0.16 | 0.013 | 0.66 | - |
| 4 | 32 | 0.47 | 0.11 | 0.009 | 0.45 | - |
| 5 | 30 | 0.5 | 0.06 | 0.005 | 0.5 | - |
| 6 | 33 | 0.45 | - | - | - | 95 |
| 7 | 23 | 0.3 | 0.16 | 0.013 | 0.9 | - |

**Table 4** Contact Surface Parameters of Each Soil Layer

| Soil layer number / parameter | 1 | 2 | 3 | 4 | 5 | 6 | 7 |
|---|---|---|---|---|---|---|---|
| $\tau_{max}$（kPa） | 20 | 20 | 22 | 35 | 62 | 75 | 55 |
| $\mu$ | 0.3 | 0.25 | 0.25 | 0.35 | 0.3 | 0.4 | 0.35 |

The thickness of the underground continuous wall is 1.8m, the thickness of the inner lining is 0.8m, the enclosure structure adopts a linear elastic model, the elastic modulus of the enclosure structure is based on the value of C30 concrete, that is, $3\times10^{10}$Pa, and the Poisson's ratio is 0.2. This paper uses the finite element software Abaqus to perform a three-dimensional finite element simulation of the circular shaft. Combined with the above working conditions, the simulation process is as follows Figure 2:

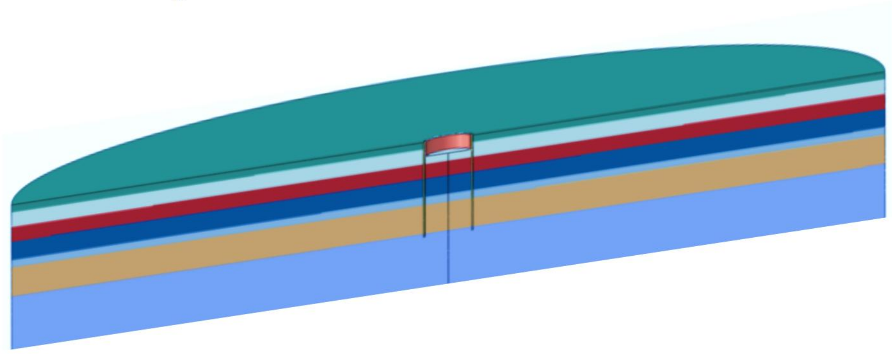

(a) Working condition 1 model

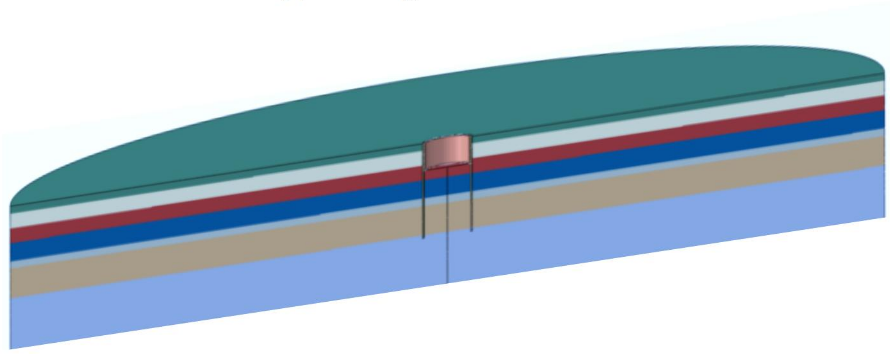

（b) Working condition 2 model

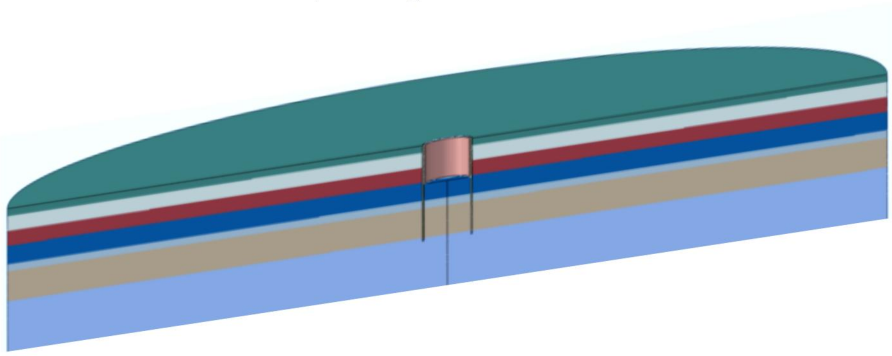

(c)Working condition three models

**Figure 2** 3D Finite Element Analysis Model of Circular Working Well

### 3.2 Analysis of Numerical Results

The calculation results and measured values of the lateral displacement of the retaining structure by three-dimensional finite element numerical simulation are shown in Figure 3. The results show that the maximum lateral displacement of the retaining structure at each excavation depth basically occurs near the excavation surface. As the excavation depth increases, the location where the maximum lateral displacement occurs also moves downward. The calculated maximum lateral displacement is consistent with the measured lateral displacement value. When the maximum excavation depth is reached, the calculated maximum lateral displacement value is 2.8 mm, and the measured maximum lateral displacement value is 3.0 mm. The ratio of the maximum lateral displacement of the wall to the excavation depth is about 0.02%, and the relative lateral displacement is small. The lateral displacement of the top and bottom of the wall is very small.

In this paper, referring to the distribution pattern of soil pressure in the Technical Code for Foundation Pit Engineering [15], the plane elastic foundation beam method considering the arch effect is used to carry out numerical simulation of the actual working condition, as shown in Figure 4. It can be seen that above the excavation surface, the lateral displacement of the retaining structure using the soil pressure distribution mode in the specification is basically consistent with the measured change trend, but there is a certain difference in the value; but below the excavation surface, the change trend of the two is different. The measured displacement value decreases with the increase of excavation depth, while the lateral displacement of the retaining structure calculated by the plane elastic foundation beam method of the soil pressure in the specification is basically unchanged below the excavation surface. There is a difference between the two, and the greater the depth, the more obvious the difference. This shows that the distribution mode of soil pressure in the existing specification cannot reflect the real deep soil pressure, and the calculation results have a certain deviation from the actual situation.

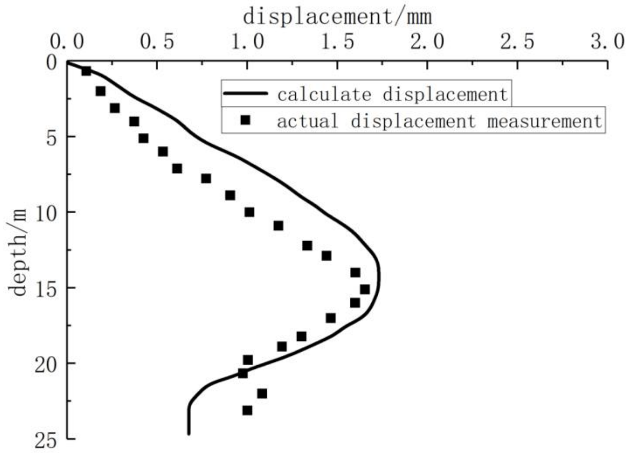


(a) working condition 1

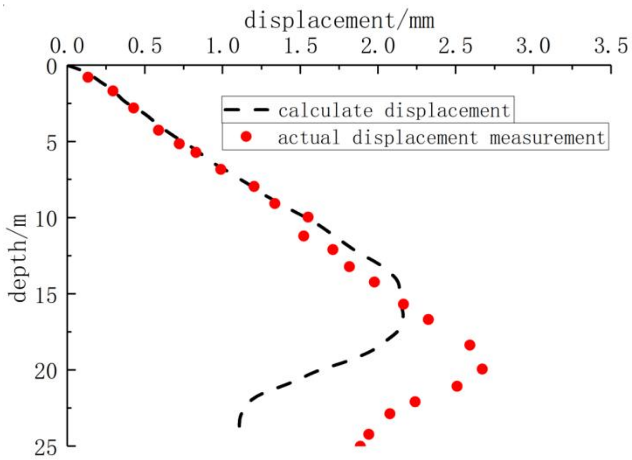


(b) working condition 2

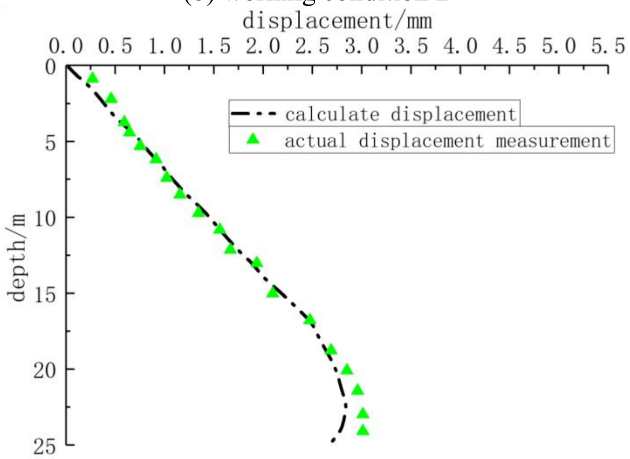


(c) working condition 3

**Figure 3** Comparison between Numerical Results and Measured Values of Lateral Displacement of Circular Working Pit Enclosure Structure

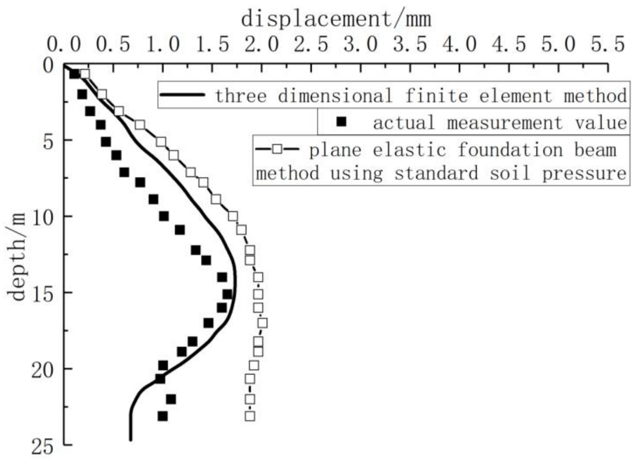


(a) working condition 1

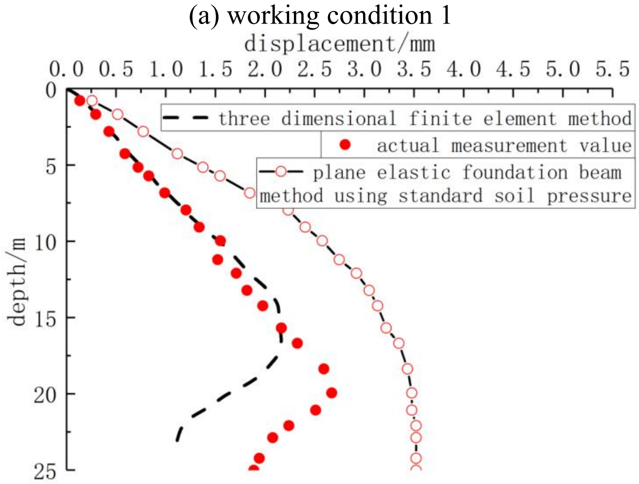


(b) working condition 2

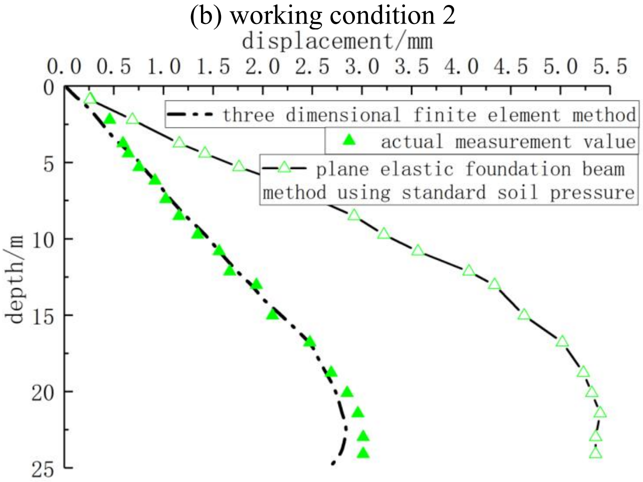


(c) working condition 3

**Figure 4** Comparative Analysis of Lateral Displacement of Circular Working Pit Enclosure Structure

## 4 SOIL PRESSURE CALCULATION METHOD CONSIDERING DISPLACEMENT EFFECT

### 4.1 Soil Pressure Calculation Model

In order to fully consider the nonlinear relationship between soil pressure and displacement of enclosure structure, the passive side and active side soil pressure relationship are established respectively:

$$P_P = P_0 + (P_{Pcrit} - P_0)\left|\frac{\Xi}{\Xi_{Pcrit}}\right| e^{\xi\left|1-\frac{\Xi}{\Xi_{Pcrit}}\right|} \quad (7)$$

$$P_A = P_0 - (P_0 - P_{Acrit})\left|\frac{\Xi}{\Xi_{Acrit}}\right| e^{\xi'\left|1-\frac{\Xi}{\Xi_{Acrit}}\right|} \quad (8)$$

In the formula, $P_P$ is the passive earth pressure; $P_A$ is the active earth pressure; $P_0$ is the static earth pressure; $P_{PC}$rit is the passive earth pressure in the limit equilibrium state; $P_{Acrit}$ is the active earth pressure in the limit equilibrium state; $\Xi$ is the wall displacement; $\Xi_{Pcrit}$ is the limit equilibrium displacement when the wall squeezes against the soil; $\Xi_{Acrit}$ is the

limit equilibrium displacement when the wall leaves the soil; ξ, ξ' are parameters related to soil properties and other factors, $0 \le \xi \le 1$, $0 \le \xi' \le 1$.
Based on the above formula, when $\Xi=0$, $P_P=P_A=P_0$; when $\Xi=\Xi_{Pcrit}$, $P_P=P_{Pcrit}$; when $\Xi=\Xi_{Acrit}$, $P_A=P_{Acrit}$, that is, the boundary conditions are met.
For any given displacement, a secant line can be drawn through the corresponding point on the curve [14], and the earth pressure can be expressed as:

$$P_P = P_0 + \Lambda_P \cdot \xi \quad (9)$$

$$P_A = P_0 + \Lambda_A \cdot \xi \quad (10)$$

In the formula, ΛP is the foundation reaction coefficient in front of the wall; ΛA is the foundation reaction coefficient behind the wall.
Further, we can get:

$$\Lambda_{\mathrm{P}} = \frac{P_{Pcrit}-P_0}{\Xi_{Pcrit}} \cdot e^{\xi\left|1-\frac{\Xi}{\Xi_{Pcrit}}\right|} \quad (11)$$

$$\Lambda_{\mathrm{A}} = \frac{P_{Acrit}-P_0}{\Xi_{Acrit}} \cdot e^{\xi'\left|1-\frac{\Xi}{\Xi_{Acrit}}\right|} \quad (12)$$

When ξ=0, ξ'=0, we can further obtain:

$$\Lambda_{\mathrm{P}} = \frac{P_{Pcrit}-P_0}{\Xi_{Pcrit}} \quad (13)$$

$$\Lambda_{\mathrm{A}} = \frac{P_{Acrit}-P_0}{\Xi_{Acrit}} \quad (14)$$

### 4.2 Analysis of Model Rationality

By comparing the soil pressure calculated by equations (7) and (8) with the three-dimensional finite element analysis model, it is found that the values and trends of the two are relatively consistent, which effectively verifies the feasibility of the three-dimensional finite element analysis model to calculate soil pressure and provides a reliable basis for subsequent research.

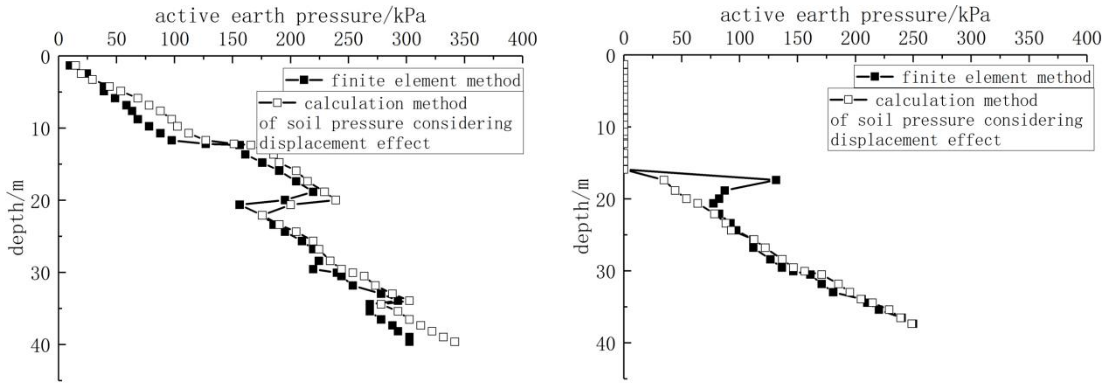


（a）active earth pressure （b）passive earth pressure

**Figure 5** Earth Pressure Distribution of Circular Working Pit Excavation (15m)

In Figure 5, the soil pressure results for each working condition are shown in Figure 6. It is found that the distribution of soil pressure below the excavation surface does not follow the constant distribution pattern of the existing specifications, but starts to decrease from a certain depth. At a certain depth, the soil pressure can be regarded as zero, and the smaller the excavation depth, the more obvious this phenomenon is.

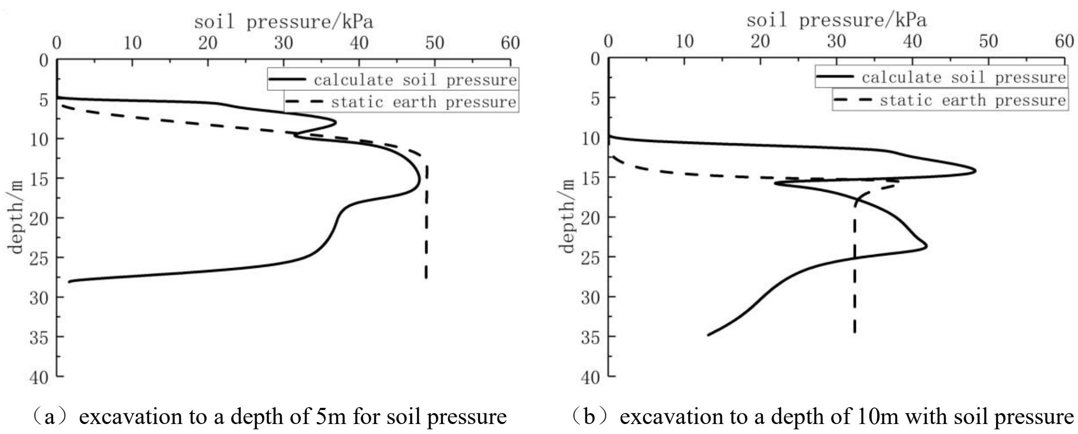


（a）excavation to a depth of 5m for soil pressure （b）excavation to a depth of 10m with soil pressure increment increment

**Figure 6** Soil Pressure Increment under Different Working Conditions of Circular Working Well

## 5 INFLUENCE OF SPATIAL ARCH EFFECT OF WORKING WELL ON SOIL PRESSURE DISTRIBUTION PATTERN

Based on the well-soil three-dimensional numerical analysis model, factors such as wall insertion ratio, working well radius, wall thickness, and wall stiffness are considered to explore the influence of spatial arch effect of working well on soil pressure distribution pattern.

### 5.1 Influence of Wall Insertion Ratio

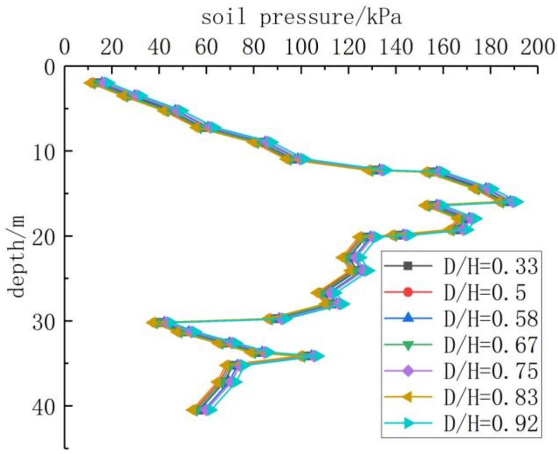


**Figure 7** Lateral Earth Pressure of Working Shaft under Different Insertion Ratios (Excavation Depth 15m)

Figure 7 shows the relationship between the lateral earth pressure of working shaft and depth when the wall insertion ratio is 0.33, 0.5, 0.58, 0.67, 0.75, 0.83, and 0.92 respectively under the premise of excavation depth 15m. It can be found that when the wall insertion ratio is changed, the change trend of the lateral earth pressure of circular shaft along the depth direction is basically the same. In other words, the size of the wall insertion ratio has little effect on the distribution pattern of lateral earth pressure of circular shaft.

### 5.2 Influence of Working Shaft Radius

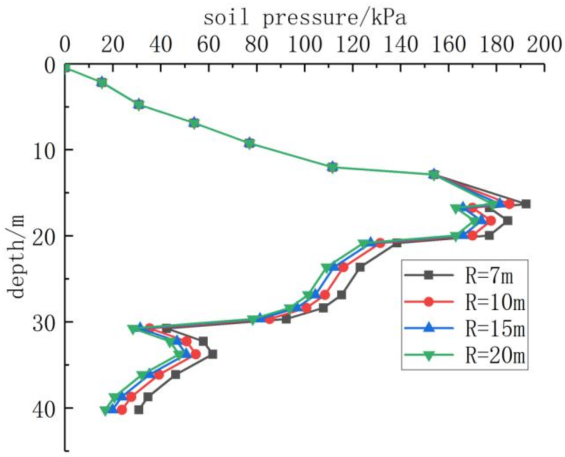


**Figure 8** Lateral Earth Pressure of Working Shaft under Different Radius Conditions (Excavation Depth 15m)

Figure 8 shows the relationship between the lateral earth pressure and depth when the working shaft radius is 7m, 10m, 15m, and 20m respectively under the premise of excavation depth 15m. As can be seen from the figure, when the radius of the working well is changed, the change trend of the lateral earth pressure along the depth direction is basically the same, and the values above the excavation surface are basically the same; but there are certain differences in the values below the excavation surface. As the radius increases, the earth pressure tends to decrease. In other words, the radius of the working well has a more prominent effect on the distribution pattern of the lateral earth pressure, and as the radius increases, the spatial arch effect becomes less obvious.

### 5.3 Influence of Wall Thickness

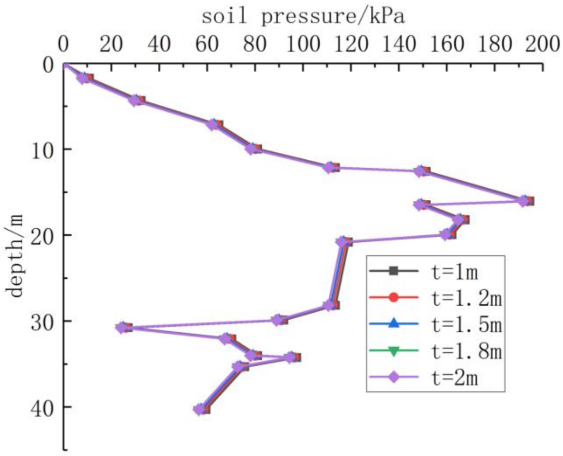


**Figure 9** Lateral Earth Pressure of the Working well under Different Wall Thickness Conditions (Excavation Depth 15m)

Figure 9 shows the relationship between the lateral earth pressure of the circular working well and the depth when the thickness of the underground continuous wall is 1m, 1.2m, 1.5m, 1.8m, and 2m respectively. The results show that when the wall thickness is changed, the change trend of the circular shaft earth pressure along the depth direction is basically the same, and the thickness change has little effect on the distribution pattern of the circular shaft earth pressure.

### 5.4 Influence of Wall Elastic Modulus

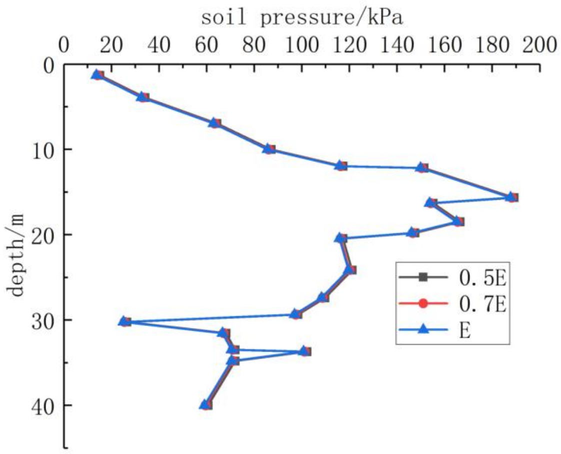


**Figure 10**. Lateral Earth Pressure of Working Shaft under Different Wall Elastic Modulus Conditions (Excavation Depth 15m)

Figure 10 shows the relationship between the lateral earth pressure of circular working shaft and depth when the elastic modulus of underground continuous wall is 0.5E, 0.7E, and E respectively. The results show that when the elastic modulus of the wall is changed, the earth pressure of the circular shaft also shows the same trend along the depth direction, and the value is almost unchanged.

## 6 CORRECTION OF EARTH PRESSURE MODEL OF CIRCULAR WORKING SHAFT IN SOFT SOIL AREA

### 6.1 Correction of Earth Pressure Distribution Model

Furthermore, the earth pressure distribution model of circular working shaft in soft soil area is studied by taking the working shaft radius as the main research factor. In view of the analysis conclusions in Section 3, the earth pressure distribution model in the existing specification [15] cannot reflect the real deep earth pressure. Therefore, it is corrected on its basis and the earth pressure distribution model of circular shaft in soft soil area is proposed. For circular working wells in soft soil areas, the distribution of soil pressure above the excavation surface is basically consistent with the distribution pattern of existing specifications; the soil pressure below the excavation surface starts to decrease from a certain depth (point A) and at a certain depth (point B), the soil pressure can be regarded as zero, and the soil pressure in the AB section is reduced linearly. The relationship between the depth of the starting point (point A) and the depth of the end point (point B) of the working wells with different radii below the excavation surface and the excavation depth and the fitting curve are shown in the figure 11 below, and the fitting formulas are obtained respectively:

$$H_{\text{Start}} = (0.019R + 1.89) \cdot H_0 \tag{15}$$

$$H_{Finish} = (0.13R + 1.95) \cdot H_0 \tag{16}$$

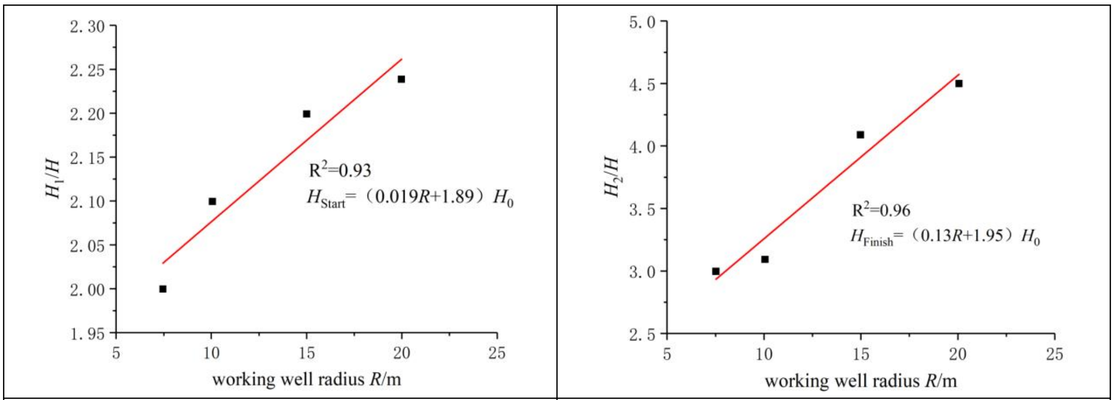


（a）starting depth of soil pressure reduction （b）end depth of soil pressure reduction

**Figure 11** Relationship between the Starting and End Depths of Soil Pressure Reduction in Circular Working Wells and Radius

### 6.2 Example Demonstration of Circular Working Wells

The actual size of the 4# circular working well in the municipal comprehensive renovation project of Shanghai Hongqiao Business District is combined with the above fitting formula to obtain the starting and end depths of soil pressure reduction, see Table 5. As shown in Figure 12, the maximum lateral displacement of the retaining structure calculated by the plane elastic foundation beam method with the modified earth pressure distribution mode is 2.0mm, which is close to the measured value of 1.7mm, 1.8mm obtained by the three-dimensional finite element method, and 2.1mm obtained by the plane elastic foundation beam method with the standard earth pressure distribution mode. However, the plane elastic foundation beam method with the modified earth pressure distribution mode is simpler to model, has more mature parameter selection, and lower calculation cost than the three-dimensional finite element method. Compared with the plane elastic foundation beam method with the standard earth pressure distribution mode, it is closer to the actual displacement trend.

**Table 5** Starting and Ending Depths of Soil Pressure Reduction

| Excavation depth $H_0$（m） | Starting depth of soil pressure reduction $H_{\text{Start}}$（m） | End depth of soil pressure reduction $H_{\text{Finish}}$（m） |
|---|---|---|
| 5 | 10.1 | 14.3 |
| 10 | 20.2 | 23（bottom of wall） |
| 15 | 23（bottom of wall） | 23（bottom of wall） |

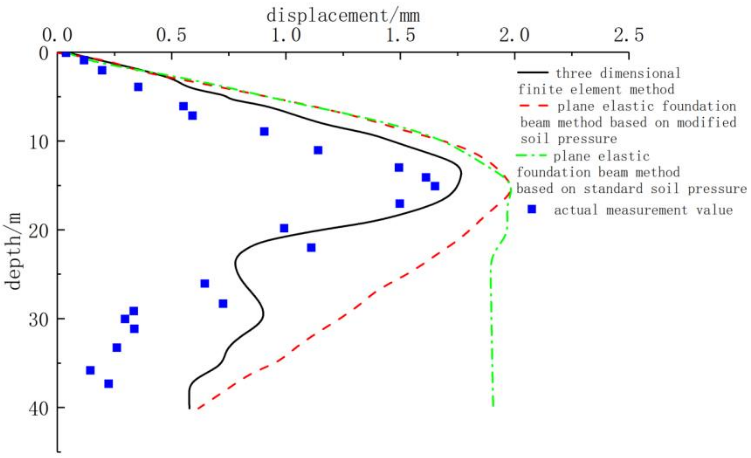


**Figure 12** Comparison of Calculated and Measured Lateral Displacements of Circular Working Well Enclosure Structure

## 7 CONCLUSION

Based on the municipal comprehensive renovation project of Shanghai Hongqiao Business District, this paper studies the soil pressure distribution pattern of circular working well in soft soil area. Based on the large-scale general finite element software Abaqus, a three-dimensional numerical analysis model of well-soil is established. Factors such as wall insertion ratio, working well radius, wall thickness, and wall elastic modulus are considered to explore the influence of the spatial arch effect of the working well on the soil pressure distribution pattern. Based on the existing specifications [15], the soil pressure distribution pattern of circular working well in soft soil area is proposed and verified by combining engineering examples. The main conclusions are as follows:

(1) Combined with the measured values, the three-dimensional numerical analysis model used in this paper can better reflect the changing trend, maximum value and corresponding position of the lateral displacement of the circular working well enclosure structure. However, the soil pressure distribution pattern in the existing specifications cannot reflect the real deep soil pressure, and there is a certain deviation between the calculation results and the actual situation.

(2) By exploring the influence of the spatial arch effect of the working well on the soil pressure distribution pattern under different influencing factors, it is found that the radius of the working well has a significant effect on it, while the wall insertion ratio, wall thickness and wall elastic modulus have little effect on it.

(3) By making corrections based on the existing specifications, the soil pressure distribution pattern of the circular working well in soft soil areas is proposed, and the fitting formula of the starting and ending depth and radius of the circular working well soil pressure reduction is obtained.

(4) By comparison, it is found that the modified earth pressure plane foundation beam method considering the circular arch effect is simpler than the three-dimensional finite element method, the parameter selection is more mature, and the calculation cost is lower. Compared with the plane elastic foundation beam method of the earth pressure in the specification, it is closer to the actual displacement trend.

## COMPETING INTERESTS

The authors have no relevant financial or non-financial interests to disclose.

## REFERENCES


[1] Tang Yeqing, Li Qimin, Cui Jiangyu. Analysis and treatment of foundation pit engineering accidents. China Architecture & Building Press, 1999.

[2] Dong Xinping, Guo Qinghai, Zhou Shunhua. Analysis of deformation characteristics and main influencing factors of circular foundation pit. Journal of Underground Space and Engineering, 2005, 1(2): 196-199.

[3] Long Minjian. Reverse construction technology of lining of large diameter vertical shaft with top pipe. Construction Technology, 2023: 176-179.

[4] Berezantzev. Axial symmetric problem of limit equilibrium of loose body (soil). Architecture & Building Society, 1956.

[5] Prater E G. An examination of some theories of earth pressure on shaft linings. Canadian Geotechnical Journal, 1977, 14(1): 91-106.

[6] Cheng Y M, Ya-Yuan H U. Active earth pressure on circular shaft lining obtained by simplified slip line solution with general tangential stress coefficient. Chinese Journal of Geotechnical Engineering, 2005, 27(1): 110-115.

[7] Liu Faqian. Study on earth pressure distribution pattern of circular foundation pit. Shanghai Jiaotong University, 2008.

[8] Mei Guoxiong, Zai Jinmin. Approximate calculation method of earth pressure considering displacement effect. Rock and Soil Mechanics, 2001, 22(1): 83-85.

[9] Zai Jinmin, Mei Guoxiong. Study on earth pressure model considering displacement. Journal of Nanjing Institute of Architecture and Civil Engineering: Natural Science Edition, 2001(1): 9-20.

[10] Zhao Jianping, Mei Guoxiong, Zai Jinmin. Study on earth pressure calculation method considering deformation and time effect. Journal of Yancheng Institute of Technology (Natural Science Edition), 2003, 16(4): 1079-1082.

[11] Lu Guosheng. Calculation method of earth pressure considering displacement. Rock and Soil Mechanics, 2004, 25(4): 586-589.

[12] Chen Yekai, Xu Riqing, Ren Chao, et al. Analysis of spatial effect of foundation pit excavation. Building Structure, 2001(10): 42-44.

[13] Chen Yekai, Xu Riqing, Yang Xiaojun, et al. Calculation method of earth pressure of flexible retaining wall in foundation pit engineering. Industrial Construction, 2001, 31(3): 1-4.

[14] Chen Yekai. Experimental study and numerical analysis of earth pressure on retaining wall. Zhejiang University, 2001.

[15] DGTJ08-61-2010, Technical Specification for Foundation Pit Engineering. Shanghai Survey and Design Industry Association, Shanghai.

[16] Roscoe K H, Schofield A N, Thurairajah A. Yielding of Clays in States Wetter than Critical. Geotechnique, 2015, 13(3): 211-240.

[17] Roscoe K H. On the generalised stress-strain behaviour of wet clay. Engineering Plasticity, 1968:535-609.

[18] DGJ08-37-2012, Geotechnical Engineering Survey Specification. Shanghai Geotechnical Engineering Survey and Design Institute Co., Ltd., Shanghai.
[19] JGJ94-2008, Technical Specification for Building Pile Foundation. Ministry of Housing and Urban-Rural Development of the People's Republic of China, Beijing.
[20] Huang Shaoming, Gao Dazhao. Soft Soil Foundation and Underground Engineering - 2nd Edition. China Architecture & Building Press, 2005.
[21] Gao D Z, Wei D D, Hu Z X. Geotechnical Properties of Shanghai Soils and Engineering Applications. ASTM, STP923, 1986, pp: 161-178.
[22] Wei Daoduo, Hu Zhongxiong. Experimental study on pre-consolidation pressure and related compressibility parameters of shallow foundation soil in Shanghai. Chinese Journal of Geotechnical Engineering, 1980, 2(4)13-22.
[23] Zhao Xihong, Jiang Hongwei, Yuan Juyun, et al. Anisotropic elastoplastic model of Shanghai soft soil. Rock and Soil Mechanics, 2003, 24(3): 322-330.
[24] Xu Zhonghua. Study on deformation characteristics of deep foundation pits combined with supporting structure and main underground structure in Shanghai. Shanghai Jiao Tong University, 2007.